Supporting Information for

The interplay between multiple doping elements in high-voltage $LiCoO_2$

Sicheng Song[a], Yiwei Li[a], Kai Yang[a], Zhefeng Chen[a], Jiajie Liu[a], Rui Qi[a], Zhibo Li[a], Changjian Zuo[a], Wenguang Zhao[a], Ni Yang[a], Mingjian Zhang[a,b], Feng Pan[a]**

[a] School of Advanced Materials, Peking University, Shenzhen Graduate School, Shenzhen 518055, People's Republic of China.

[b] Center for Advanced Radiation Source (ChemMatCARS), the University of Chicago, Argonne, Illinois 60439, United States.

*Corresponding author: zhangmj@pkusz.edu.cn (M.Z.); panfeng@pkusz.edu.cn (F.P.);

1. Figures

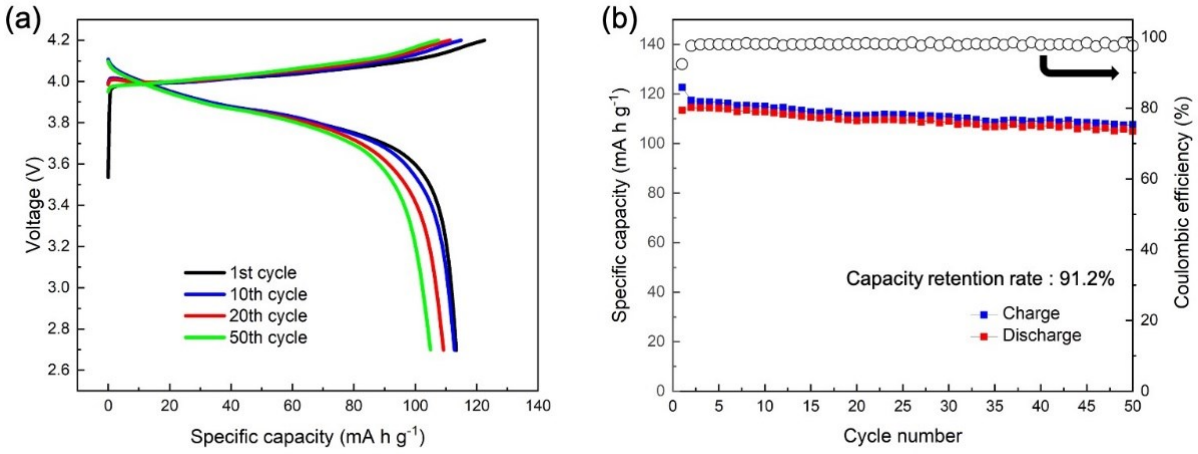

Figure S1. Electrochemical performance of LCO in the voltage range of 2.7-4.2 V using the current density of 150 mA g^{-1}. (a) The charge/discharge profiles at selected cycles. (b) The cycling performance of LCO.

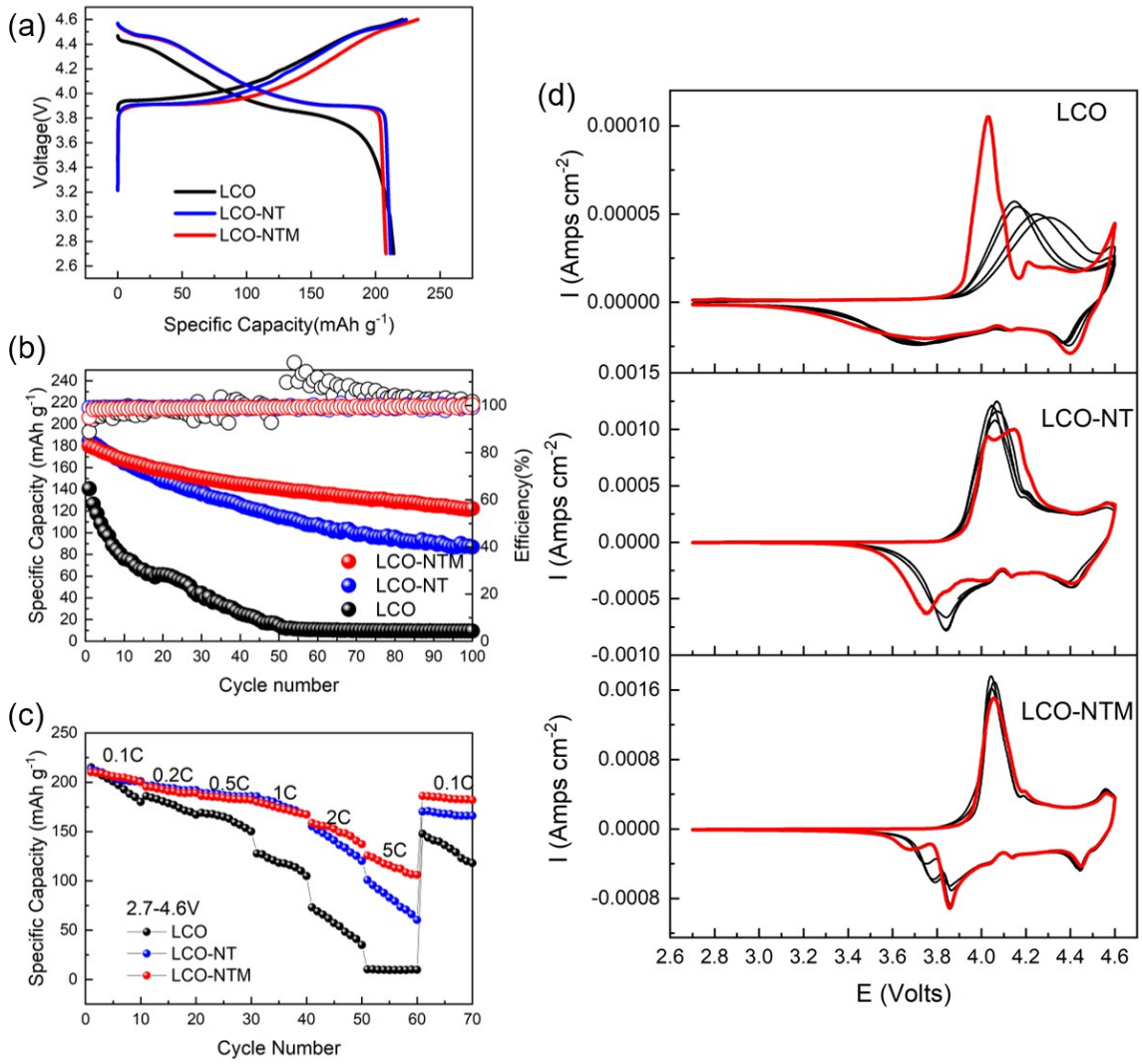

Figure S2. Electrochemical characterization of LCO and co-doped LCO in the voltage range of 2.7-4.6 V. (a) The first charge–discharge voltage profiles at 0.1 C. (b) The cycling performance at 1 C. (c) Rate performance. (d) The CV curves of LCO, LCO-NT and LCO-NTM in the initial five cycles.

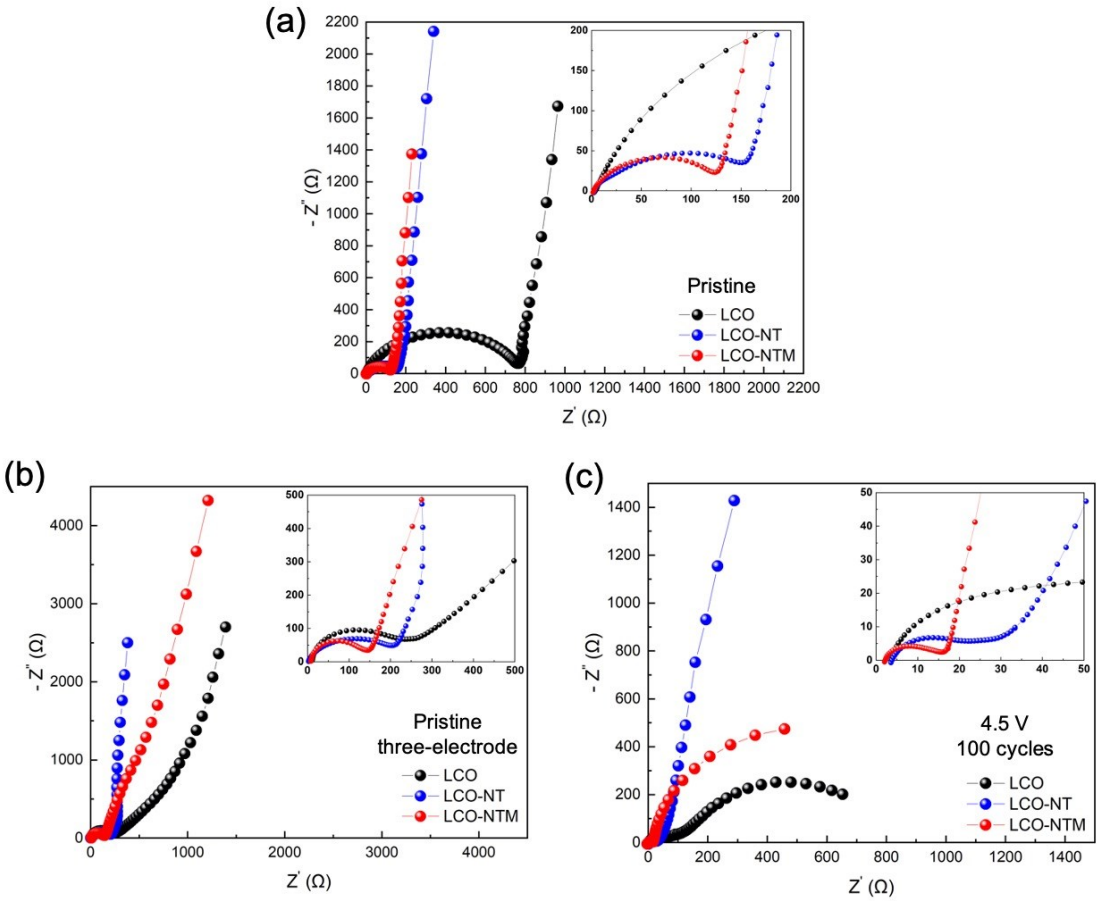

Figure S3. Electrochemical impedance spectra for LCO, LCO-NT and LCO-NTM cathodes, respectively, before cycling using coin-cell setup (a), before cycling using three-electrode setup (b), and after 100 cycles using coin-cell setup (c). In the three-electrode setup, Pt electrode and Ag/AgCl electrode were used as the work electrode and the reference electrode, respectively.

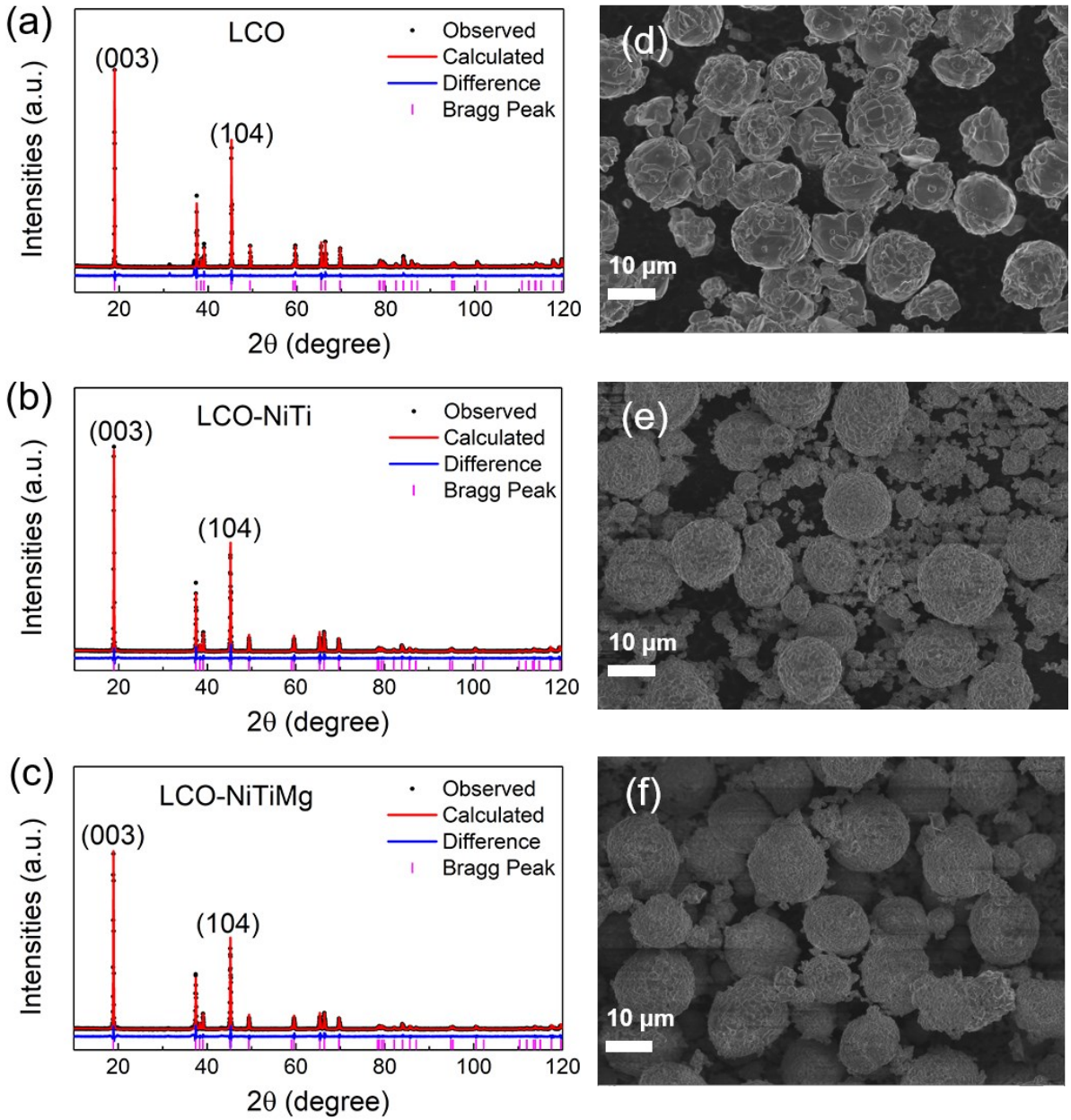

Figure S4. XRD patterns and Rietveld refinements of LCO (a), LCO-NT (b) and LCO-NTM (c). scanning electron microscope (SEM) images of LCO(d), LCO-NT (e) and LCO-NTM (f).

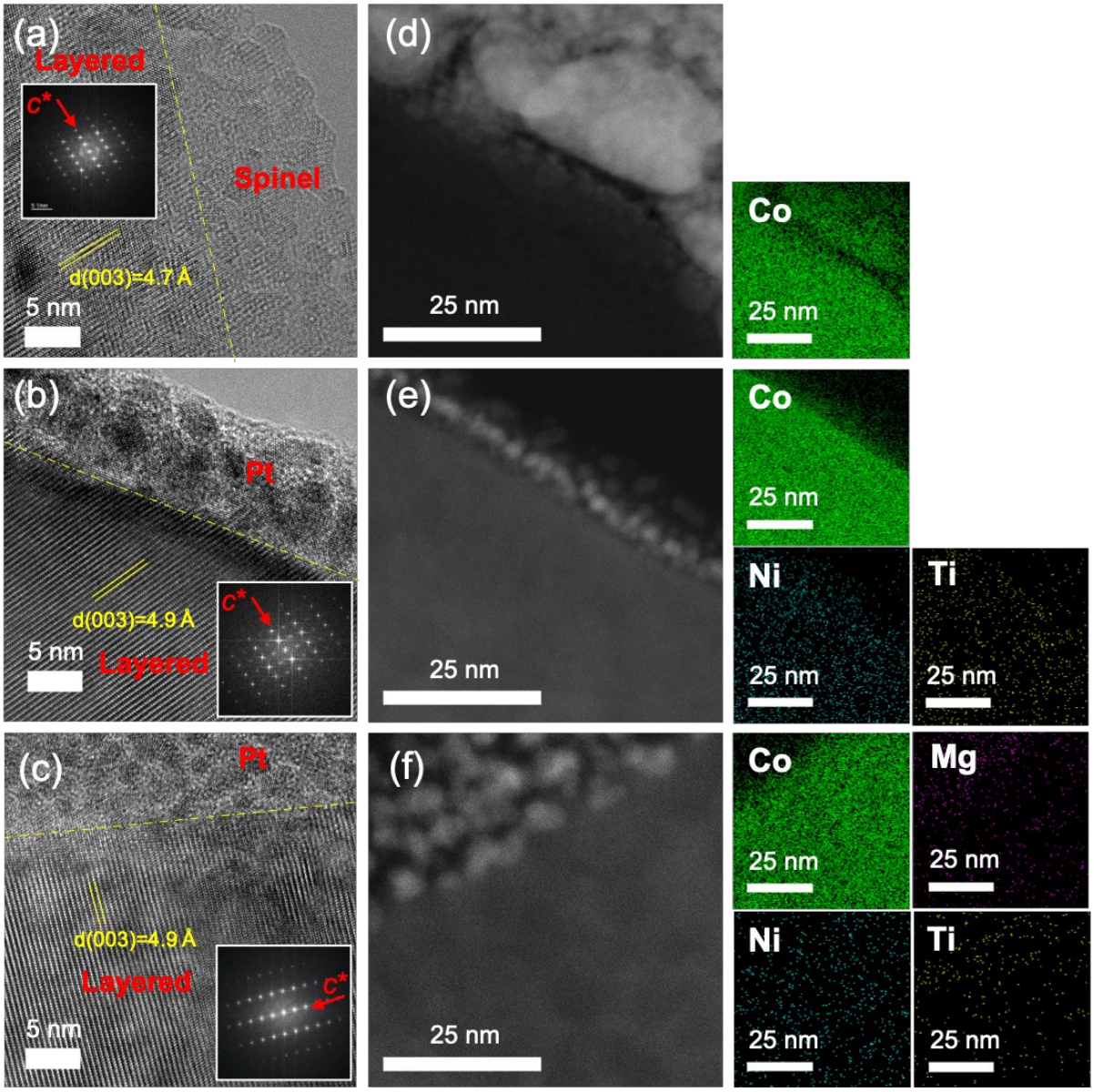

Figure S5. HRTEM images at the particle surface of LCO (a), LCO-NT (b) and LCO-NTM (c). The corresponding TEM-EDX mapping of LCO (d), LCO-NT (e) and LCO-NTM (f).

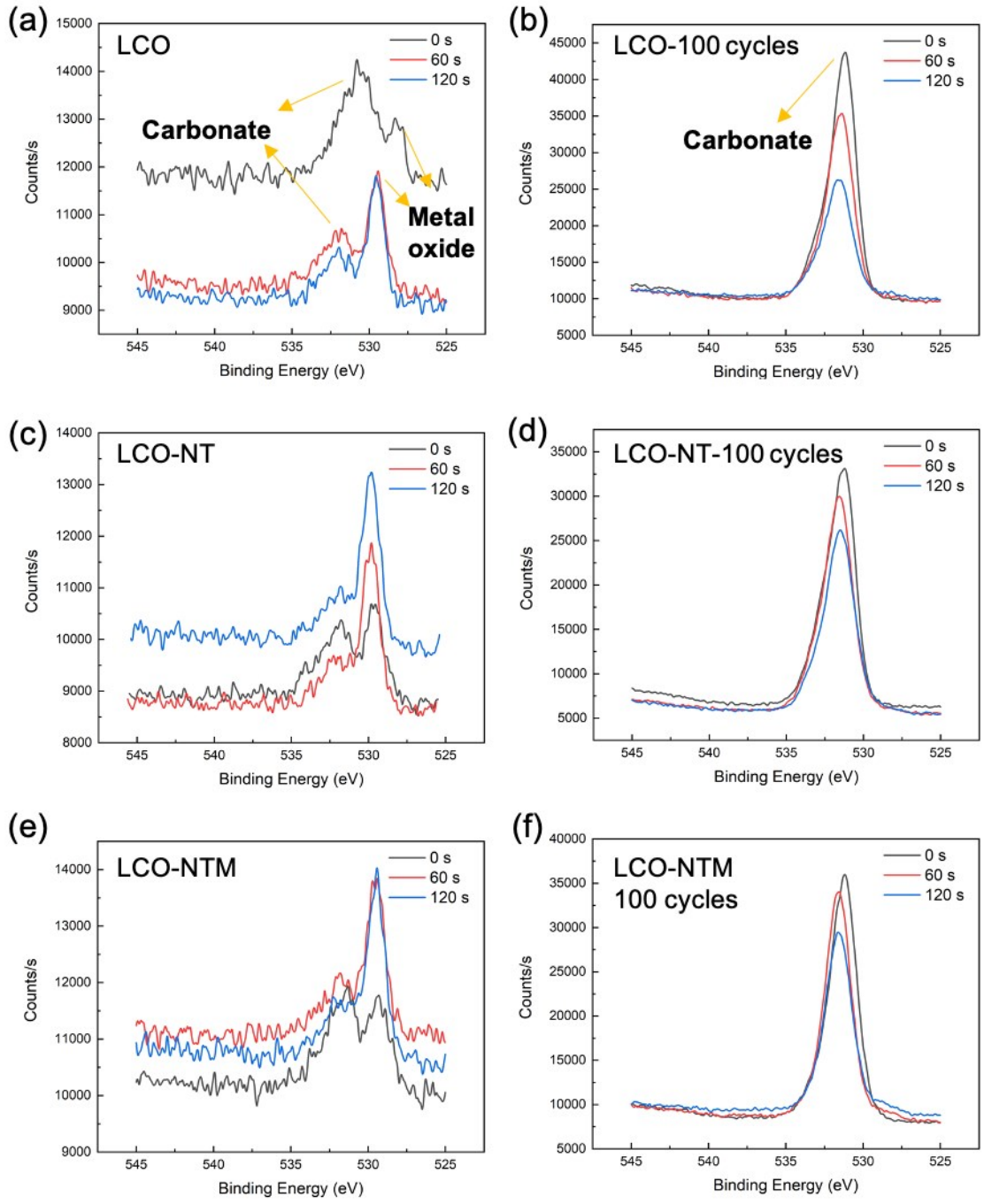

Figure S6. O 1*s* spectra of LCO (a, b), LCO-NT (c, d), and LCO-NTM (e, f) before cycling and after 100 cycles.

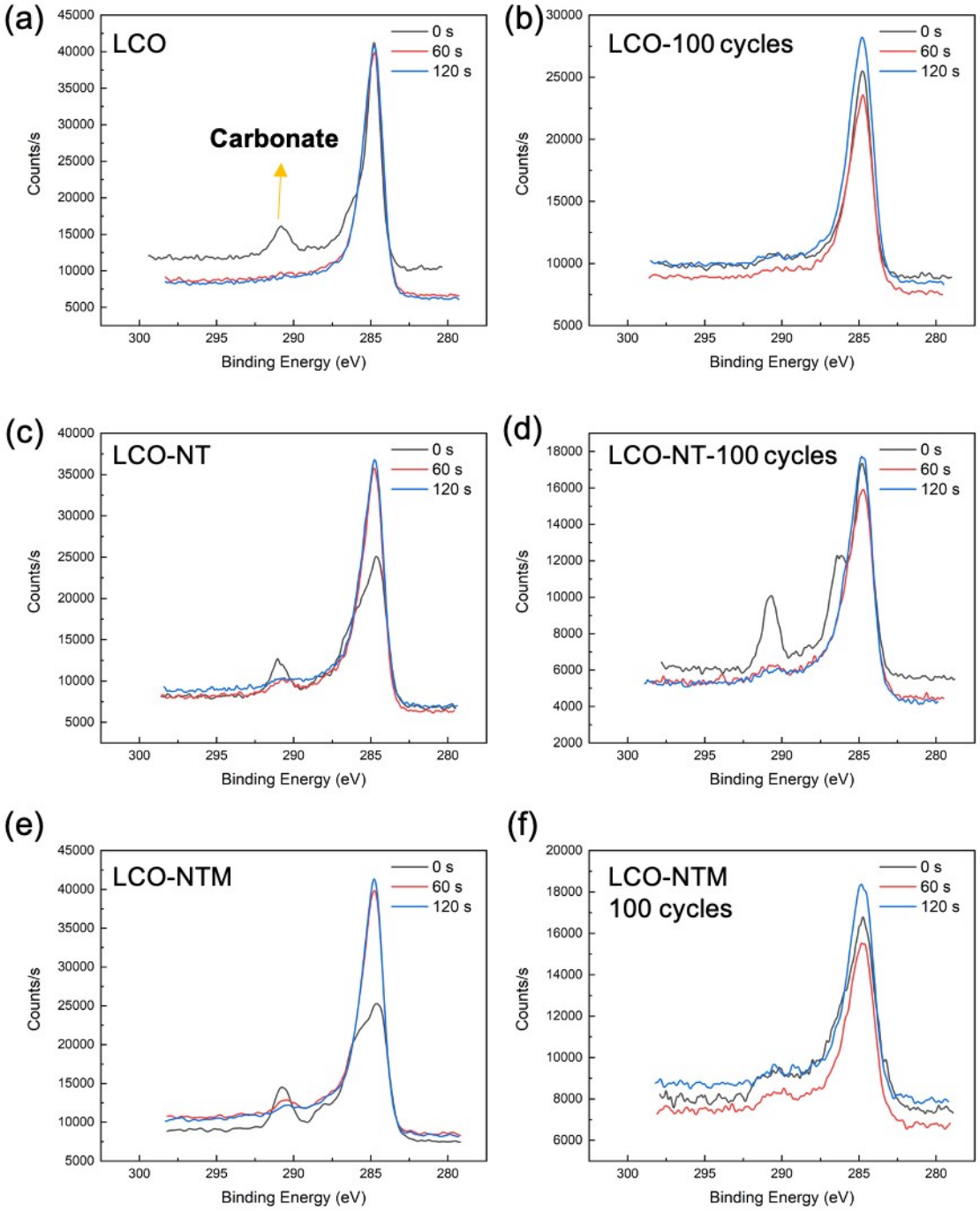

Figure S7. C 1*s* spectra of LCO (a, b), LCO-NT (c, d), and LCO-NTM (e, f) before cycling and after 100 cycles.

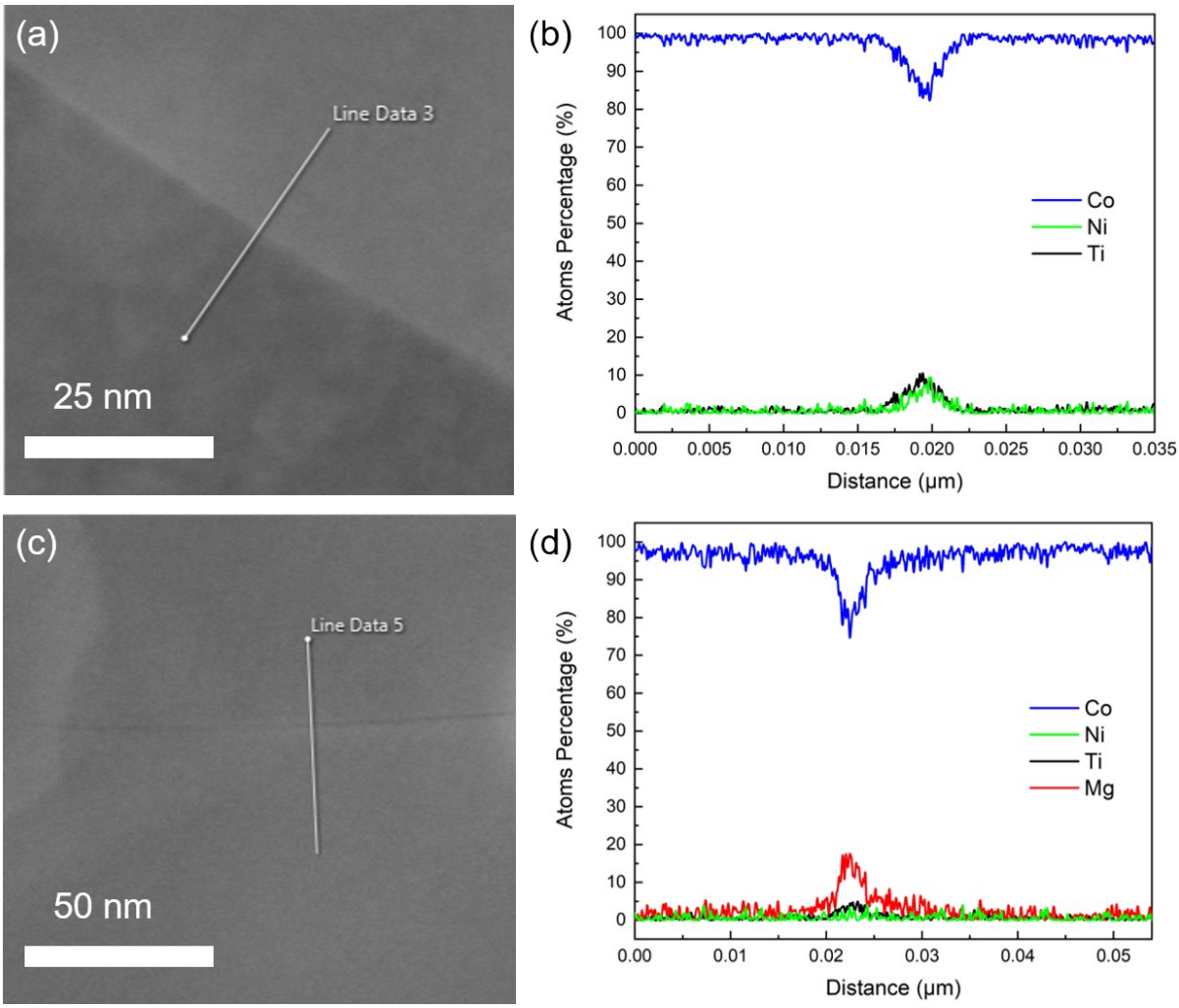

Figure S8. TEM images of the grain boundaries for LCO-NT (a) and LCO-NTM (c). EDX line scanning of LCO-NT (b) and LCO-NTM (d) perpendicular to the grain boundary in the corresponding TEM images (labelled by the white lines). The total content of all metal elements is normalized to 100%.

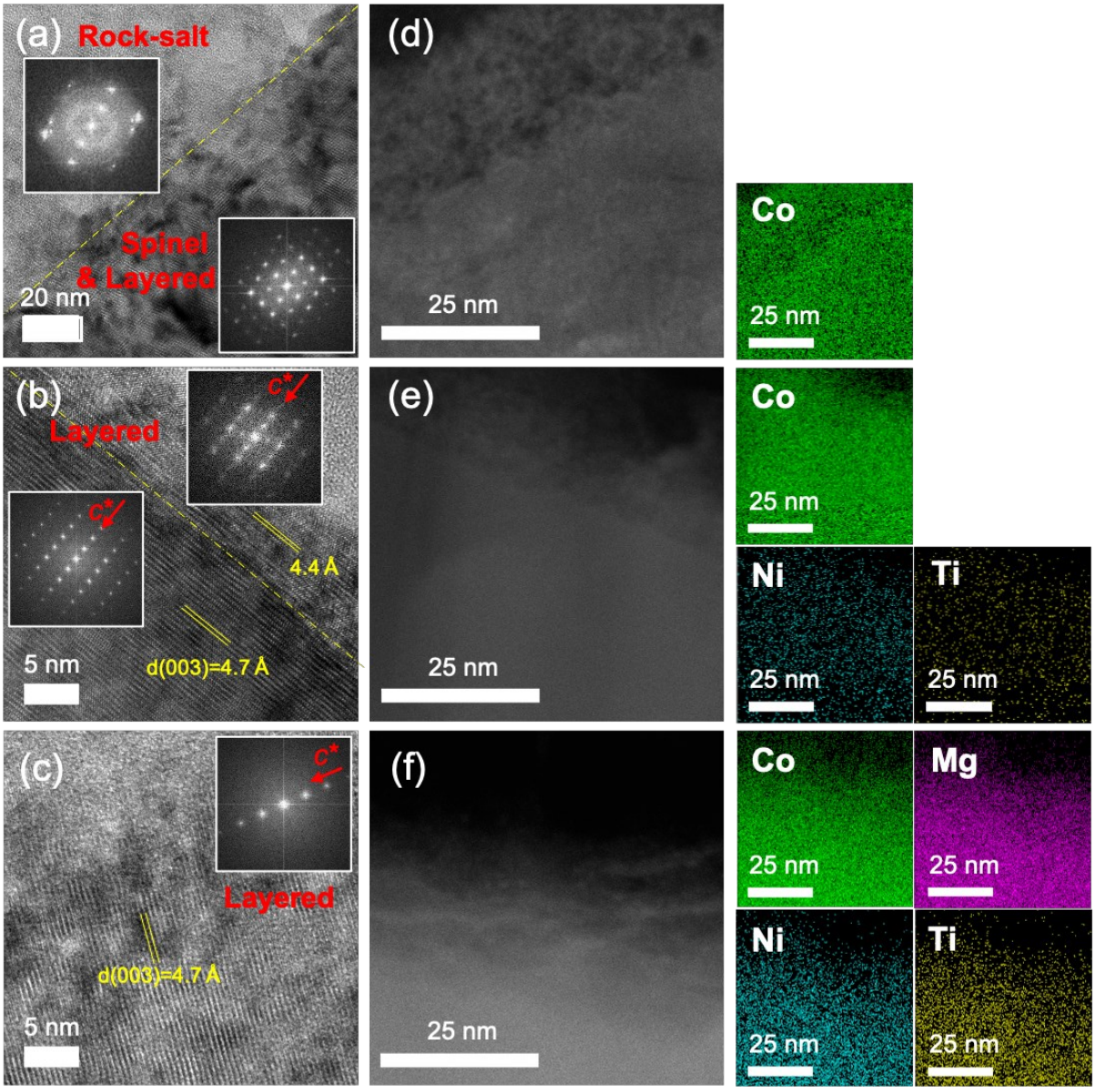

Figure S9. HRTEM images at the particle surface of LCO (a), LCO-NT (b) and LCO-NTM (c) after 100 cycles at 4.5 V. The corresponding TEM-EDX mapping of LCO (d), LCO-NT (e) and LCO-NTM (f) after 100 cycles at 4.5 V.

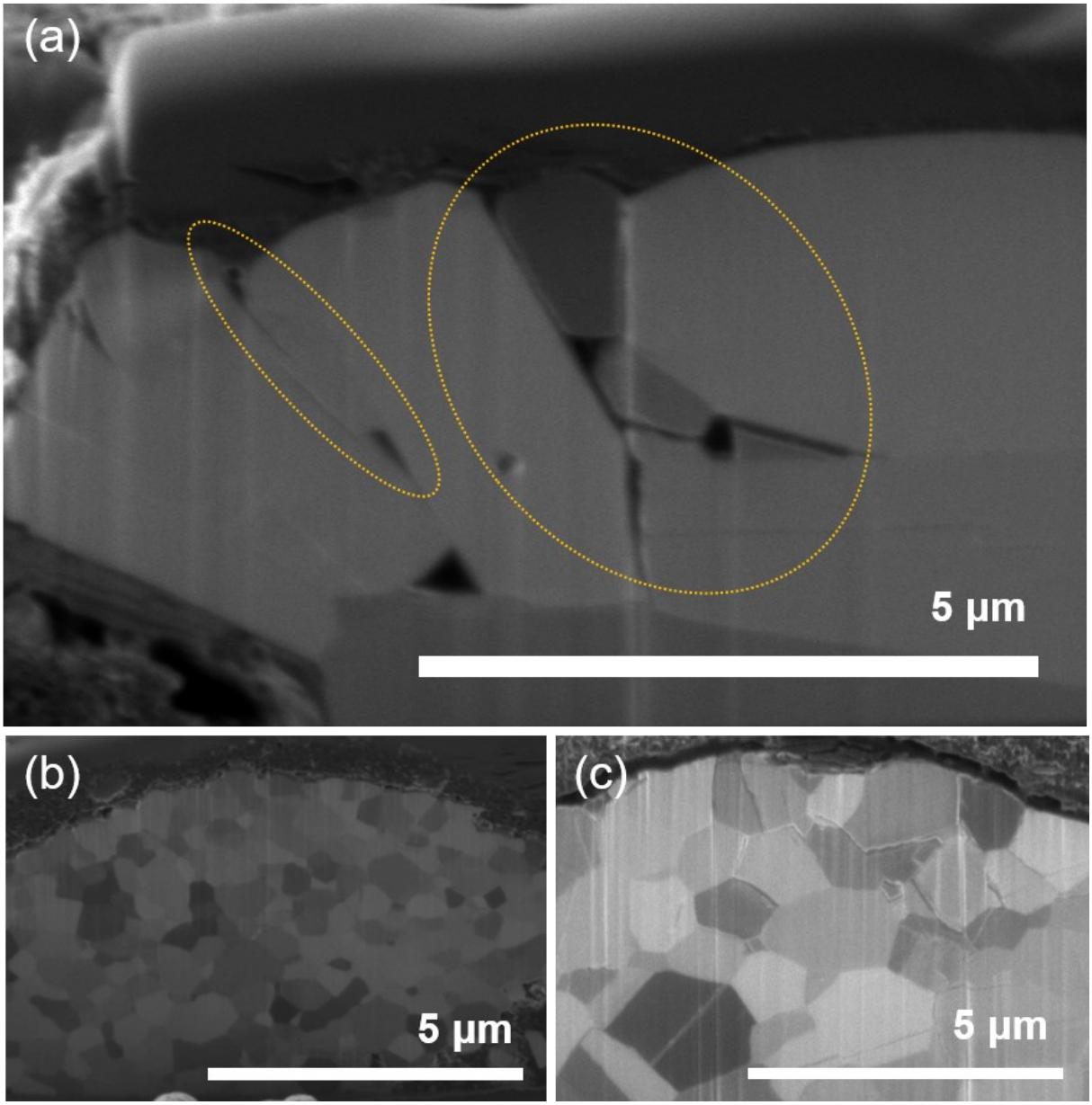

Figure S10. Ion-induced secondary electron (ISE) images of the cross sections for LCO (a), LCO-NT (b) and LCO-NTM (c) after 100 cycles at 4.5 V. The cross-section samples were prepared by FIB.

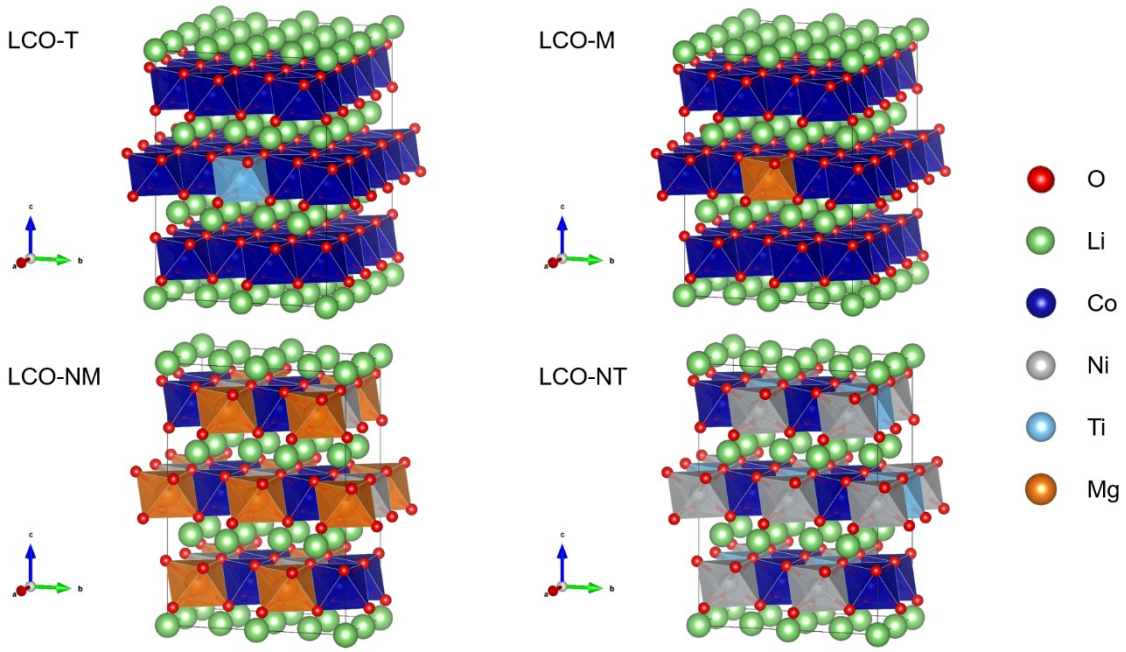

Figure S11. Structure models of Ti doped LCO (LCO-T), Mg doped LCO (LCO-M), Ni/Mg co-doped LCO (LCO-NM) and Ni/Ti co-doped LCO (LCO-NT) for DFT calculations.

2. Tables

Table S1. The elemental compositions determined by ICP-AES. The sum of Co, Ni, Ti, Mg was normalized to 1.0. The Li content was normalized accordingly.

Sample	molar ratio				
	Li	Co	Mg	Ni	Ti
LCO	1.0504	1.000	-	-	-
LCO-NT	1.0609	0.9830	-	0.0071	0.0099
LCO-NTM	1.0615	0.9688	0.0111	0.0097	0.0102

Table S2. Refinement parameters for XRD patterns of LCO, LCO-NT and LCO-NTM.

Samples	LCO	LCO-NT	LCO-NTM
Space group	*R*-3*m*	*R*-3*m*	*R*-3*m*
R_{wp}	4.02	4.92	4.59
R_p	2.48	3.04	3.05
a (Å)	2.815194(17)	2.814625(28)	2.814282(33)
c (Å)	14.05060(14)	14.07512(24)	14.07566(28)
V (Å^3)	96.4366(15)	96.5659(25)	96.5461(30)
grain size (nm)	457(10)	247.2(39)	217.5(35)
z(O)	0.24153(18)	0.24154(17)	0.24141(18)
Li-slab (Å)	2.5798(19)	2.5840(34)	2.5878(36)
TM-slab (Å)	2.1038(28)	2.1077(27)	2.1041(30)

Table S3. The BET surface areas for three samples.

Samples	BET surface area ($m^2 g^{-1}$)
LCO	0.5113
LCO-NT	0.0113
LCO-NTM	0.0291

Table S4. The calculated total energies (E_{total}), formation energies (E_f) and the lattice parameter *c* of eight structure models in Figure 6a and S10.

Compounds	Structural models	E_{total} (eV)	E_f (eV/atom)	*c* (Å)
LCO	$Li_{48}Co_{48}O_{96}$	-227295.378	-2.9919	13.077
LCO-N	$Li_{48}Co_{47}NiO_{96}$	-227798.420	-2.9867	13.083
LCO-T	$Li_{48}Co_{47}TiO_{96}$	-225175.048	-2.9340	13.100
LCO-M	$Li_{48}Co_{47}MgO_{96}$	-225095.915	-3.0164	13.081
LCO-NT	$Li_{24}Co_{12}Ni_6Ti_6O_{48}$	-104032.479	-3.1579	13.433
LCO-TM	$Li_{24}Co_{12}Mg_6Ti_6O_{48}$	-87822.279	-3.5651	13.588
LCO-NM	$Li_{24}Co_{12}Ni_6Mg_6O_{48}$	-103474.161	-3.2766	13.315
LCO-NTM	$Li_{24}Co_6Ni_6Mg_6Ti_6O_{48}$	-90839.312	-3.4903	13.468

Notes. The atomic energies for Li, Co, O, Ni, Ti and Mg are -190.9905，-3676.6141，-427.8742，-4180.6497，-1567.3877，-1472.4343 eV, respectively.

Table S5. The formation energies (E_f) of four systems: (1) the coexistence of LCO and LCO-NTM; (2) the coexistence of LCO-N and LCO-TM; (3) the coexistence of LCO-T and LCO-NM; (4) the coexistence of LCO-M and LCO-NT.

Four cases	E_f(eV/atom)
6 LCO + LCO-NMT	-3.0302
6 LCO-N + LCO-TM	-3.0312
6 LCO-T + LCO-NM	-2.9604
6 LCO-M + LCO-NT	-3.0273